CIMAC CONGRESS 25
ZURICH, MAY 19 – 23, 2025

2025 | 098

Challenges of measuring raw exhaust of ammonia engines

Controls, Automation, Measurement, Monitoring & Predictive Maintenance

Philipp Jakubec, IAG Test Cell Technology GmbH

ABSTRACT

Society is moving towards climate neutrality where ammonia-fueled combustion engines (NH_3 - ICE) could be considered a main technology. These engines run on ammonia (NH_3) so carbon-based emission are only present at a very low level from the lube oil. The most important pollutants NO and NO_2 are caused by the exhaust aftertreatment system as well as CO_2 coming from the ambient air. What challenges current emission measurement systems is measuring unburnt ammonia in high levels as well as high water content.

For standard measurement technologies these low levels of CO_2 are hard to detect due to the high water content. Normal levels of CO_2 are between 400-500 ppm which is very close or even below the detection limit of commonly used non-dispersive-infrared-detectors (NDIR). Equally, the high water content is very challenging for NOx measuring devices, like chemiluminescence detectors (CLD), where it results in higher noise and therefore a worse detection limit. Even for Fourier-transformed-infrared-spectroscopy-analysers (FT-IR), it is challenging to deal with water content over 15% without increased noise. In the past ammonia measurements in high levels were never requested so this technology must be evaluated from the beginning.

The goal of this study was to show that measuring low levels of CO_2 and NOx as well as high levels of ammonia can be performed by FT-IR. Therefore, new calibrations are created, considering that water levels might be above 25 Vol%. These were first tested by calibration gases in wet and dry conditions. Afterwards a two-stroke single-cylinder engine that is run on ammonia was used to generate real engine data. The FT-IR analyzer was compared with theoretical data as well as against other analyzers. Several steady-state points as well as different load cycles were performed.

The results show a large improvement in reducing the noise caused by high water and therefore a more accurate measurement at low concentrations. High ammonia readings can be achieved without any loss in accuracy and without any interference coming from water. Ongoing tests are performed to see if the calibrations can be further approved.

1 INTRODUCTION

Future legislation in the major engine markets of Europe, China, America and Japan will cut down the emission limits of pollutants such as carbon dioxide (CO_2), carbon monoxide (CO) and nitrogen oxides (NO_x). The upcoming regulations might also require nitrous oxide (N_2O) and ammonia (NH_3) to be measured. All these components can be quantified by state-of-the-art analytical devices which are widely available. Of course, devices that are able of measuring all of them at once are preferable. One of these suitable multi-gas devices is the Fourier-Transformed-Infrared-Spectrometer (FTIR) which will be used in this work.

To achieve these new goals alternative fuels will play a big role. One of the most important ones for large engines will be ammonia, either used as a blend with other fuels or as a total replacement of them. Both options have advantages as well as challenges. Diesel blends are already well known for their robustness and are easy to manufacture in large scales. Pure NH_3-ICEs show very good results regarding their emissions in large engine applications. Due to their thermal efficiency and short refueling time NH_3-ICE can be taken into account as a prime technology to achieve climate neutrality as targeted by the EU until 2050.[2]

The objective of this paper is to improve the measurement accuracy of FTIR technology used on a NH_3 fueled ICE. Therefore, it will also be compared to other analytical devices like chemiluminescence detectors (CLD) or non-dispersive-infrared-detectors (NDIR). Especially unburnt ammonia together with high water content will be observed.

2 THEORETICAL BACKGROUND

2.1 Ammonia Engine

2.1.1 Challenges of Ammonia Engines

Ammonia (NH_3) is increasingly considered a potential alternative fuel for internal combustion engines (ICEs) and fuel cells due to its carbon-free nature, high energy density, and potential for integration with renewable energy systems. Despite these advantages, several challenges need to be addressed before ammonia can be widely adopted as an engine fuel. These challenges range from combustion issues, environmental concerns, and safety risks, to technological barriers related to ammonia production and utilization. This section will explore these challenges in detail, focusing on the main aspects that hinder the effective use of ammonia in engine applications.

2.1.2 Combustion Characteristics

One of the primary technical challenges associated with ammonia as a fuel in internal combustion engines is its combustion characteristics. Ammonia has a higher ignition temperature (around 650°C to 700°C) than traditional fuels like gasoline or diesel, which makes it more difficult to ignite. The high ignition temperature is due to the strong bonds between nitrogen and hydrogen in the ammonia molecule, which require a greater amount of energy to break. Consequently, conventional spark plugs or compression ignition techniques may not be sufficient for efficient combustion of ammonia in internal combustion engines.

This issue necessitates modifications to existing engine designs. For example, engines may need to incorporate advanced ignition systems, such as pre-chamber ignition or plasma-assisted ignition, which can provide higher temperatures or more energy to initiate the combustion of ammonia. Furthermore, the high ignition temperature can result in incomplete combustion or misfire issues, reducing engine efficiency and performance.

Additionally, ammonia's wide flammability limits (15.5% to 33% by volume in air) and low volatility at ambient temperatures complicate the control of combustion, leading to difficulties in optimizing the air-fuel mixture for stable operation. Achieving a uniform distribution of ammonia within the combustion chamber is also critical to avoid the formation of hotspots, which can lead to engine knock and other operational problems.

2.1.3 Nitrogen Oxides (NO_x) Emissions

Another significant challenge in ammonia combustion is the formation of nitrogen oxides (NO_x), which are harmful pollutants. NO_x is a byproduct of the high-temperature combustion process that occurs when ammonia breaks down in the presence of oxygen. The formation of NO_x is a concern because these compounds contribute to air pollution, acid rain, and respiratory issues. While ammonia does not produce carbon dioxide (CO_2) during combustion, which makes it attractive as a carbon-free fuel, NOx emissions must still be managed.

Ammonia combustion can lead to the formation of both NO and NO_2, with NO being the primary pollutant. The formation of NO_x depends on factors such as combustion temperature, pressure, and the oxygen-to-fuel ratio.

- **Thermal NOx**: This mechanism is driven by the high combustion temperatures required for ammonia combustion. Nitrogen in the air reacts with oxygen at elevated temperatures (above 1500°C) to form NO and NO_2. Ammonia, when introduced into the combustion chamber, can exacerbate the formation of NOx due to the high temperature requirements for ignition and combustion.

- **Prompt NOx**: The prompt mechanism involves the reaction of hydrocarbons with nitrogen present in the combustion chamber. While ammonia does not contain hydrocarbons, the use of ammonia may still lead to the formation of trace hydrocarbons, potentially facilitating the prompt NOx formation pathway.

In addition, ammonia's higher molecular weight and specific heat can lead to local temperature peaks in the combustion chamber, further exacerbating NOx formation.

To mitigate these emissions, ammonia engines may need to employ advanced emission control technologies, such as selective catalytic reduction (SCR) or exhaust gas recirculation (EGR), which are commonly used in diesel engines. These systems can reduce NOx emissions by converting nitrogen oxides into harmless nitrogen and water vapor, but they add complexity and cost to the engine system.

2.1.4 Unburnt ammonia emissions

Unburned ammonia, often referred to as "ammonia slip," represents another significant emission from ammonia-powered engines. Ammonia slip occurs when the combustion process is incomplete, resulting in residual ammonia in the exhaust gases. The factors influencing ammonia slip include engine load, air-to-fuel ratio, combustion temperature, and engine speed. Incomplete combustion can result in the release of ammonia into the atmosphere, which is detrimental to air quality and can contribute to the formation of fine particulate matter (PM) and secondary pollutants such as ammonium nitrate (NH_4NO_3).

The ammonia slip is particularly pronounced under low-load and lean-burn conditions, where combustion temperatures are insufficient to completely break down ammonia.

2.1.5 Carbonaceous emissions

One of the key advantages of ammonia is its carbon-free nature, meaning that it does not produce carbon dioxide (CO_2) during combustion. This significantly reduces the GHG emissions compared to conventional fuels like diesel or gasoline. However, ammonia combustion may still produce other pollutants, including particulate matter (PM) and trace hydrocarbons, depending on the combustion process and engine configuration.

2.1.6 Energy Efficiency and ammonia cracking

Ammonia's high energy density is one of its most attractive features as a fuel, but the practical use of ammonia in internal combustion engines or fuel cells requires overcoming additional efficiency hurdles. For example, in ammonia-powered fuel cells, ammonia must first be cracked into hydrogen before it can be used in the fuel cell. Ammonia cracking involves a catalytic process where ammonia is decomposed into nitrogen and hydrogen gases. The hydrogen can then be used in the fuel cell to generate electricity. However, the process of cracking ammonia is energy-intensive, requiring significant thermal or electrical input.

At present, ammonia cracking systems are not highly efficient, and this inefficiency reduces the overall energy return from ammonia as a fuel source. The process also typically requires high temperatures (around 800°C to 1000°C) and specific catalysts, adding to the complexity and cost of ammonia-based energy systems. Additionally, the need for ammonia cracking may negate some of the environmental benefits of using ammonia as a carbon-free fuel if the cracking process is powered by fossil fuels or if it leads to additional energy losses.

The inefficiency of ammonia cracking is particularly problematic for portable or mobile applications, such as ammonia-powered vehicles. In these applications, weight and space constraints demand high-efficiency fuel systems, which current ammonia cracking technologies do not adequately provide.

2.1.7 Ammonia storage and safety

Ammonia is a toxic and corrosive substance, presenting significant safety challenges in its use as a fuel. It has a strong odor and is highly hazardous if inhaled in high concentrations, leading to respiratory problems, eye irritation, and other health issues. Furthermore, ammonia is corrosive to metals, requiring special materials for fuel tanks, pipes, and engine components.

Storing ammonia safely is another significant issue. While ammonia is easier to store than hydrogen, it still requires pressurized or refrigerated conditions to remain in liquid form at ambient temperatures. This introduces additional challenges for developing fuel storage systems that are both safe and efficient. In some cases, ammonia must be stored in specially designed tanks capable of withstanding high pressures (typically around 8-10 bar) or low temperatures, which adds to the overall system weight and complexity.

Moreover, the risk of ammonia leakage is a critical safety concern. Any leak or rupture in an ammonia storage system can lead to toxic exposure to humans and the environment. Strict safety measures must be in place to prevent leaks and ensure that ammonia is handled correctly, particularly during refueling operations. This need for rigorous safety protocols adds to the cost and logistical complexity of implementing ammonia-based energy systems.

2.1.8 Infrastructure and distribution

The infrastructure required for ammonia production, storage, and distribution must also be considered when adopting ammonia engines on a large scale. Although ammonia is already widely produced for agricultural purposes, the infrastructure for handling ammonia as a transportation fuel is not yet in place. Transporting ammonia in bulk requires specialized vessels, pipelines, or trucks, and the need for refueling stations equipped to handle ammonia safely presents another significant logistical challenge.

The widespread use of ammonia engines would require a substantial investment in new infrastructure to ensure a reliable and accessible supply of ammonia for vehicles, ships, and power plants. Additionally, the carbon footprint associated with ammonia production—primarily through the Haber-Bosch process—must be addressed to ensure that the environmental benefits of ammonia as a fuel are fully realized. If ammonia is produced using fossil fuels, it could negate some of its potential benefits in reducing global greenhouse gas emissions.

- **Strategies for emission control**
  Selective Catalytic Reduction (SCR) is one of the most widely researched and employed methods for controlling NOx emissions in ammonia-fueled engines. SCR systems utilize a catalyst to reduce NOx emissions by injecting a reducing agent, such as ammonia or urea, into the exhaust gas. The ammonia reacts with NOx at a catalyst surface, converting them into nitrogen and water. However, careful control of the ammonia-to-NOx ratio is critical to avoid ammonia slip and ensure the efficiency of the SCR system**.**
- **Exhaust Gas Recirculation (EGR)** is another promising strategy for controlling NOx emissions in ammonia combustion. EGR works by recirculating a portion of the exhaust gas back into the combustion chamber. This reduces the oxygen concentration and lowers the peak combustion temperature, thereby reducing NOx formation. Combined with advanced combustion strategies, EGR can help mitigate NOx emissions and improve the overall efficiency of ammonia-fueled engines.
- **Advanced combustion technologies**

  The adoption of advanced combustion techniques, such as lean-burn combustion, dual-fuel configurations (ammonia and hydrogen), and optimized spark timing, can help reduce both NOx and ammonia slip. By reducing the combustion temperature and optimizing the air-to-fuel ratio, these techniques minimize the conditions that promote NOx formation while ensuring complete ammonia combustion.

2.2 FTIR

Fourier-transformed-infrared spectroscopy measures infrared absorption of a gas. It collects data with a resolution of high over a broad spectral range simultaneously. Therefore, it contains an infrared radiation source, a Michelson-Interferometer, a He-Ne reference laser and a detector. Figure 1 shows a schematic sketch of a FTIR measurement stem.

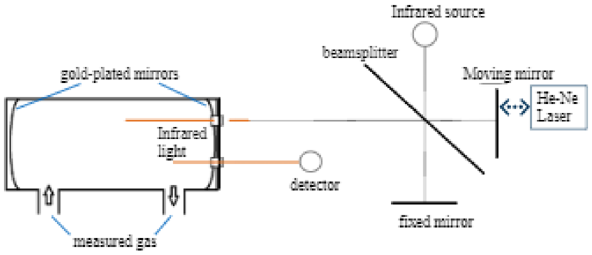

Figure 1: Schematic sketch of the measurement chamber and Michelson-Interferometer

The reference laser (He-Ne) is used to measure the position of the moveable mirror of the Michelson-Interferometer. This mirror is sensitive to vibrations or other mechanical impact which makes it necessary to permanently measure the actual position.

The detector is made of Mercury-Cadmium-Telluride (MCT) and requires liquid-nitrogen cooling. Therefore, the observed spectral range reaches from 500-6000 cm^{-1} with a resolution of 0.5 cm^{-1}. This increases the sensitivity, especially for lower wavenumbers.

The infrared light is split by a beam splitter into two beams. A fixed and a moving mirror each reflect one beam. After reflection, both beams are connected again to interfere. The interference is depending on the position of the moveable mirror. That means, the interferogram results with its maximum where both mirrors have been in the same distance to the beam splitter. The interferogram is turned into a spectrum by Fourier-transformation.

The sample gas streams through a stainless-steel measurement chamber with gold plated, MgF_2 coated mirrors on both ends. These mirrors reflect the infrared light to a pathlength of 5.11 m, which is the most used one in engine applications. It is able to cover ranges from ppm to several Vol%. The infrared light enters and leaves the measurement chamber though Zinc Selenide (ZnSe) windows. Since the size of this chambers has a big impact on the response time a small 70 ccm chamber is used. The data were collected with 5 Hz.

Nearly all components of exhaust gas absorb infrared light which makes FTIR very effective to use for engine testing. Typically, molecules with a small energy difference between the rotational and vibrational state absorb infrared light very well. The quality of the absorption is depending on the change of the dipole moment in a molecule while vibrating or rotating. The only molecules not possible to measure are molecules like N_2, H_2 or O_2. They do not have a changing dipole moment while they undergo rotational or vibrational motions. As a result, they cannot absorb infrared light making them invisible for FTIR-analysis. In Figure 2, an example of a background sample, when the measurement chamber contains Nitrogen only, is shown. The y-axis is denoted in unitless quantity -Absorbance Units. The absorbance defines as "the logarithm of the ratio of incident to transmitted radiant power through a sample (excluding the effects on cell walls)".[3]

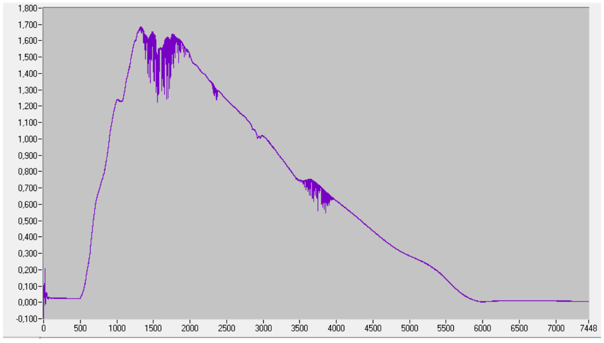

Figure 2: Background spectrum of a FTIR

During measurements this spectrum is subtracted from the currently measured one. This results in peaks of absorbed infrared light. Figure 3 shows the subtracted spectrum of a NH_3-ICE.

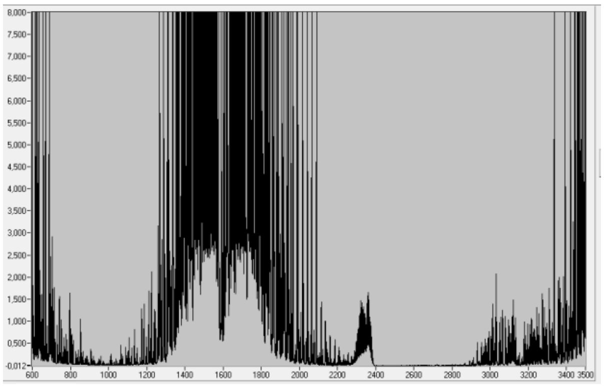

Figure 3: Substraced spectum of ammonia – ICE

Each component has a specific shape and wavenumber area where it is absorbed. This fact is used to create calibrations via the Beer-Lambert-Law:

$$A = \varepsilon * c * d$$

Equation 1: Beer - Lambert – Law

A	Absorption
ε	absorption coefficient at a specific wavelength
C	Concentration of component
D	Optical path length of the measurement chamber

Table 1: Beer - Lambert - Law definitions

The absorption coefficient is specific for each molecule. It describes the extent of absorbing infrared light at a specific wavenumber. To check for potential cross sensitivities spectra of single components are needed. Due to the fact that each component has its characteristic line shape and region where its absorption is present. Of course, most of these regions are not unique to a single component. In fact, most components share regions with others. To ensure the detection of only the observed component single-gas spectra are put on top of each other to search for gas-specific areas. In figure 4 an example is shown for H_2O (red) and CO_2 (white). A region where only CO_2 is present is chosen.

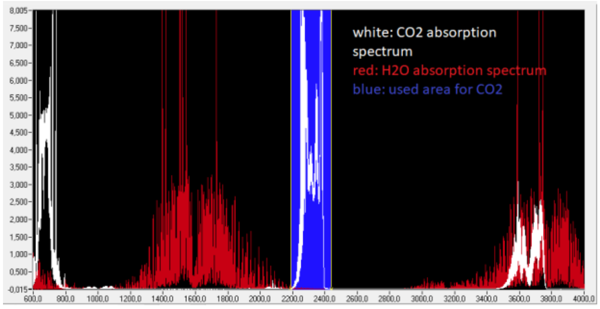

Figure 4: Wavenumber area

This must be done for all gases that might be present in the exhaust stream to avoid cross sensitivities. Since the line shape and areas of infrared absorption are highly reproduceable if the temperature and pressure are kept at certain levels it is possible the build libraries for different fuel types.

To ensure that pressure and temperature are permanently controlled and adjusted if needed the FTIR was built in a IAG Versa06 measuring device. It regulates the pressure to 1 atm (± 0.05 atm) and the temperature to 191 °C (± 2 °C). It takes care about filtration and sample handling (f.e. flow control) as well.

Table 2 provides a not complete list of measured components in the original library, used at the beginning of the tests.

Measured component	Detection Limit	Calibration Range
CO	1,9 ppm	10 Vol%
CO_2	144 ppm	20 Vol%
NO	2,0 ppm	3000 ppm
NO_2	0,9 ppm	300 ppm
N_2O	0,6 ppm	300 ppm
CH_4	1,5 ppm	5000 ppm
H_2O	320 ppm	25 Vol%
NH_3	1,2 ppm	3000 ppm
C_2H_2		1000 ppm
C_2H_4O		1000 ppm
C_2H_6		1000 ppm
C_2H_4		1000 ppm
CH_2O		500 ppm

Table 2: Gases measured by FTIR

2.3 Standard **exhaust gas analyzers**

So-called standard exhaust components are still often measured with the devices specified in table 3. For carbon monoxide (CO) and carbon dioxide (CO_2) a non-dispersive infrared detector (NDIR) is used. Nitrous oxides (NO_x) are measured by a chemiluminescence detector (CLD).[4] These types of analyzers are still state-of-the-art. In this study a AVL AMA i60 is used.

Measured component	Principle	Calibration Range
NO_2	CLD	3000 ppm
NO_x	CLD	3000 ppm
CO_2	NDIR	20 Vol%
CO	NDIR	10 Vol%

Table 3: Gases measured by standard analyzer

A NDIR analyzer contains an infrared source, a sample chamber a light filter and an infrared detector. The infrared light is sent through the sample chamber towards the detector. The exhaust gas causes absorption which can be measured by the detector. An optical filter in front of the detector eliminates all light except the chosen wavelengths for CO_2 and CO. NDIR analyzers suffer from high cross sensitivity to water.[4] Therefore, the engine-out exhaust gas is dried by a cooler before entering device. Since the FTIR is measuring on a wet basis the CO and CO_2 readings must be corrected to either wet or dry. Due to the easier availability of water measurements by the FTIR all values used in this work are dry. If wet values are used for some reason it is mentioned. The calculate dry values formula 2 is used.

$$CO_x\,(dry) = \frac{CO_x(wet)}{(100 - H_2O\ [Vol\,\%])/100}$$

Equation 2: Wet - Dry correction

CLD analyzers measure the light emitted by exited NO_2 atoms returning to their ground state. Therefore, the NO_x molecules from the exhaust gases must be transferred into an exited state to be able to emit light. Then the emitted light is proportional to the NO/NO_x concentration in the exhaust stream. CLD analyzers usually work with dry sample gas similar to the NDIR[5]. However, there are analyzers working with wet sample gas streams. These tend to underreport NO_x levels as the water vapor can quench the chemiluminescence effect[6].

2.4 Experimental Setup

To start building the improved calibrations for NH_3, NO and NO_2 single cylinders at different concentrations were used to create a satisfying number of single gas spectra. The used bottles are specified in table 4. As a carrier gas nitrogen (N_2) 5.0 was used.

Component	Supplier	Accuracy	Range
NO	Messer	± 1%	9000 ppm
NO	Messer	± 1%	500 ppm
NO_2	Messer	± 1%	300 ppm
NH_3	Messer	± 1%	1000 ppm
NH_3	Messer	± 1%	8 Vol%

Table 4: List of used gas bottles

These gas bottles were connected to an IAS HovaCal gas divider. This was used to have the ability of creating humidified test gases. The gas divider was connected to the IAG Versa06 by a 3m heated line to prevent condensation. The setup is shown as a sketch in figure 5.

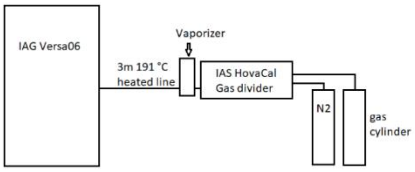

Figure 5: Sketch of gas divider setup

Since the expected water content is high compared to standard Diesel engines the calibration was improved as well.

The finalized calibrations were tested on spark-ignited single cylinder engine that was adapted to run on ammonia fuel.

3 BUILDING CALIBRATIONS

3.1 NO Calibration development

A 500 and a 9000 ppm NO bottle were used together with a gasdivider to create 52 raw spectra, starting from 0ppm with steps of 50 ppm until 1000 ppm, after that the steps are performed with 250 ppm. This indicates that the calibration will have a range of 9000 ppm. The data were collected with an IAG Versa06 FTIR system at 1 atm and 191 °C with a flow of 5 l/min at 10 Hz. An average of 1 min was used to minimalize the noise.

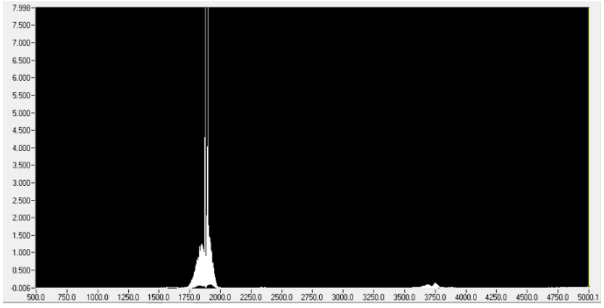

Figure 6: Absorption spectrum of 9000 ppm NO

If the region from 1750 cm^{-1} to 200 cm^{-1} is observed with a closer look it shows some total absorbed peaks in the middle part. All peaks that are higher than 2.5 AU can be considered as totally absorbed. Therefore, this region will be cut out, which is indicated in figure 7.

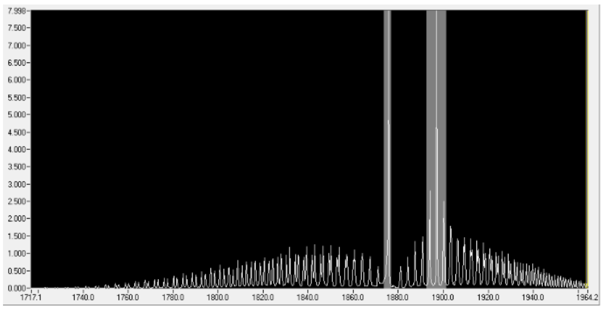

Figure 7: Used absorption regions for 9000 ppm NO

Only the black parts of the spectrum are used. These are is calculated separately for all 52 spectra, ranging from 0 to 9000 ppm. Since the exact concentration of each spectrum is known a fourth order polynom can be created to match the calculated concentration with the actual one.

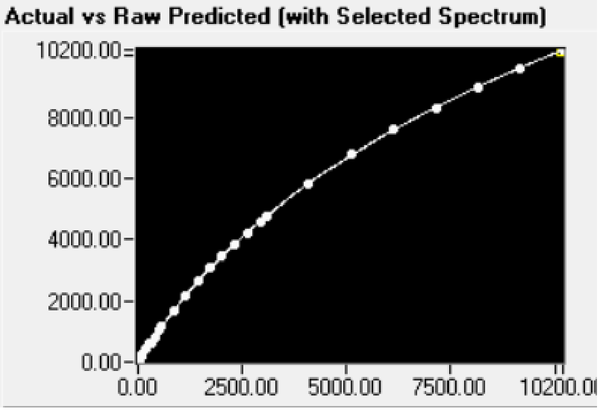

Figure 8: Actual vs predicted NO concentration

In this case the polynom resulting a coefficient of determination of 0.9997.

3.2 NO_2 Calibration development

A 300 ppm NO_2 bottle was used to create 20 spectra with 15 ppm steps.

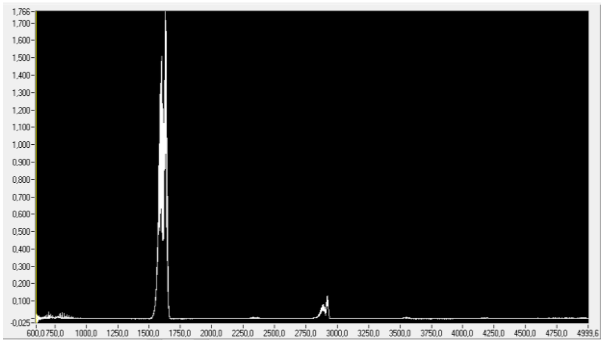

Figure 9: Absorption spectrum of 300 ppm NO_2

Here both regions could be used for creating a calibration. Due to the higher peaks the region from 1500 to 1670 cm^{-1} is chosen.

The same way of calculating a polynom is used again, resulting in a linear interpolation with a R^2 of 0.9998.

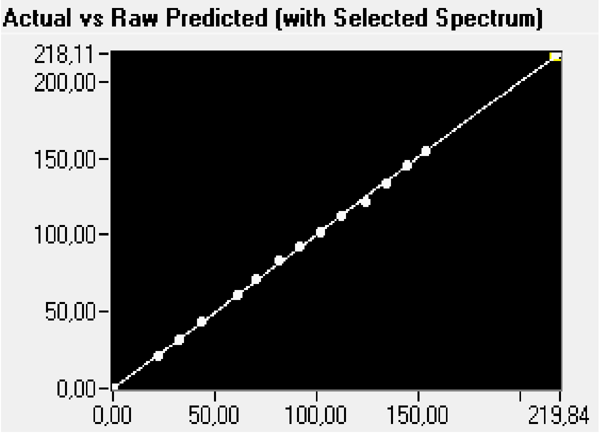

Figure 10: Actual vs predicted NO_2 concentration

3.3 NH_3 Calibration development

Since unburnt fuel will lead to a level several percentage ammonia in the exhaust stream, a completely new ammonia calibration was created.

A 1000 ppm and a 8 Vol% calibration gas bottle were used to create 111 files with step sizes of 100 ppm up to 2000 ppm, 250 ppm up to 5000 ppm 1000 ppm up to 8 Vol% of ammonia.

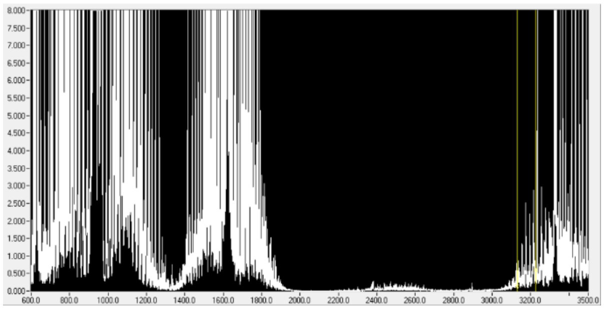

Figure 11: Absorption spectrum of 8 Vol% ammonia

Since most regions are saturated at these high levels a very small region was used to create the calibration.

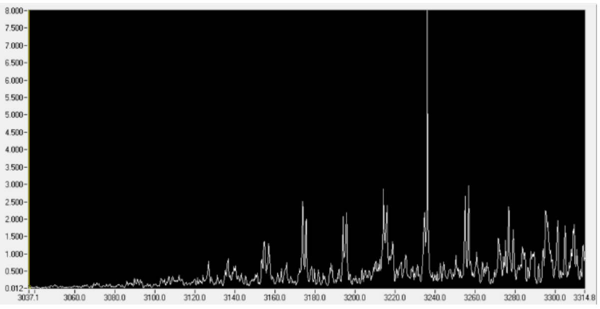

Figure 12: Used absorption region for 8 Vol% ammonia

For this calibration a cubic polynom was used that a achieved a R^2 of 0.9997.

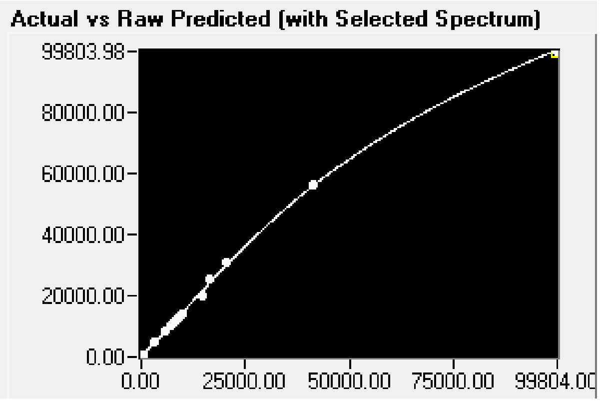

Figure 13: Actual vs predicted ammonia concentration

3.4 H_2O Calibration development

When ammonia is used as a fuel the expected water concentration will be higher than in conventional diesel engines. Therefore, the calibration was extended to 40 Vol%. Since vaporized water cannot be stored in conventional gas bottles, distilled water was vaporized with an IAS HovaCal MFC gasdivider.

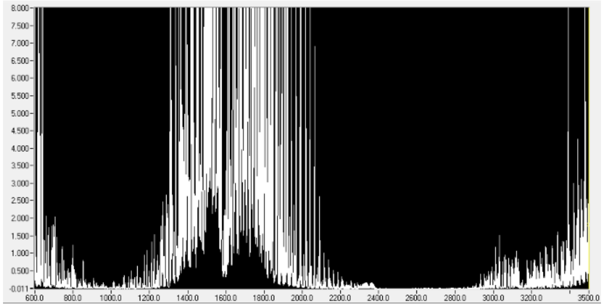

Figure 14: Absorption spectrum of 40 Vol% H_2O

Again, due to saturation a specific region must be picked.

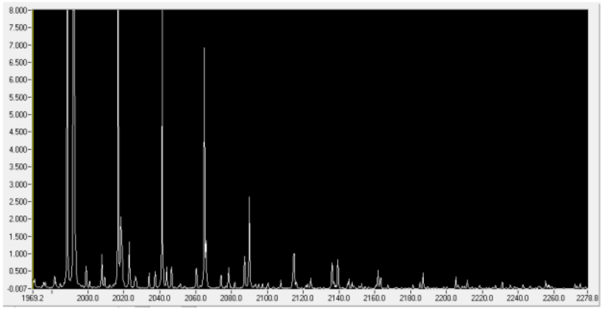

Figure 15: Used absorption spectum of 40 Vol% water

In this case a 4th degree polynom was used to create the calibration. It results in a coefficient of determination of 0.9997.

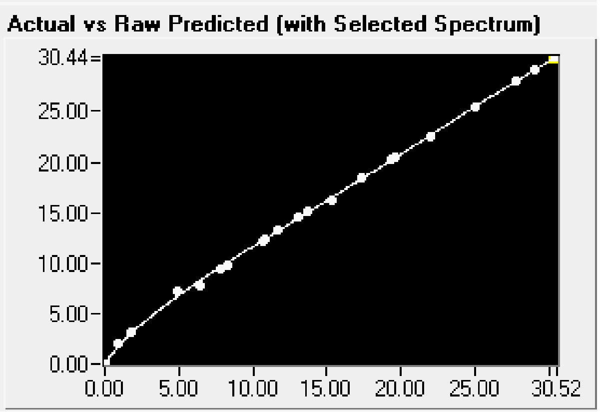

Figure 16: Actual vs predicted water concentration

3.5 Checking for cross sensitivities

As mentioned above peak areas might not be exclusive for one component. Therefore, a gas matrix of CO, CO_2, H_2O, NH_3, NO, N_2O, Methane (CH_4) and Propane (C_3H_8) was created with an IAS HovaCal. The spectra of this mixture were collected as well and plotted against the new calibrations for NO, NO_2, NH_3 and H_2O.

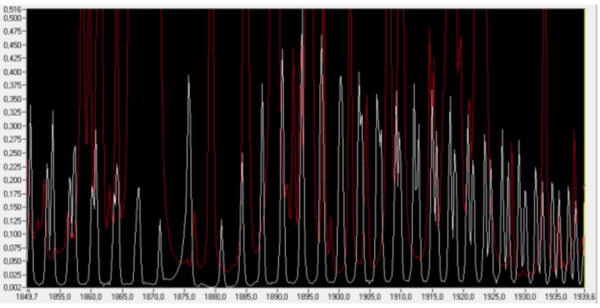

Figure 17: Absorption peaks of 1000 ppm NO (white) plotted against gas matrix (red)

It is clearly visible that most NO peaks are not exclusive and are covered by the gas matrix. To avoid potential miss-interpretation only the few specific peaks are used for the final calibration and linearization.

The same spectra were plotted against our NO_2 calibration.

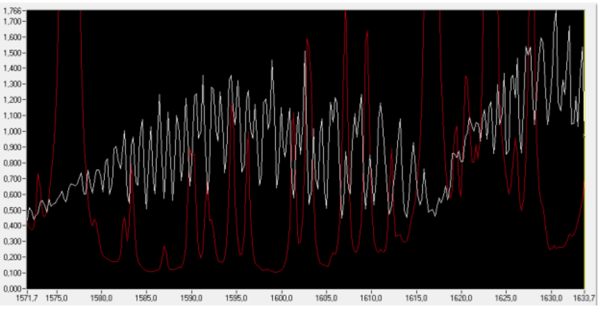

Figure 18: Absorption peaks of 200 ppm NO2 (white) against gas matrix (red)

Again, several areas must be excluded from our calibration. The exclusive peaks are used to do the calculation again and the polynom was adjusted.

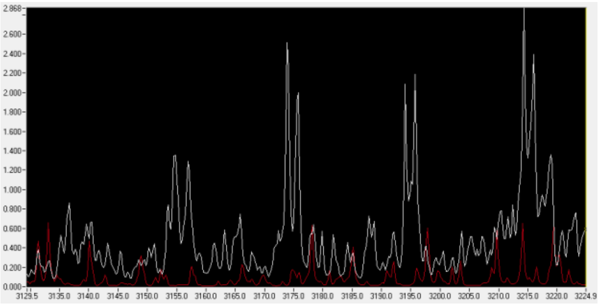

Figure 19: Absorption peaks of 8 Vol% NH3 (white) against gas matrix (red)

The new ammonia calibration is checked as well, and some areas have to be removed.

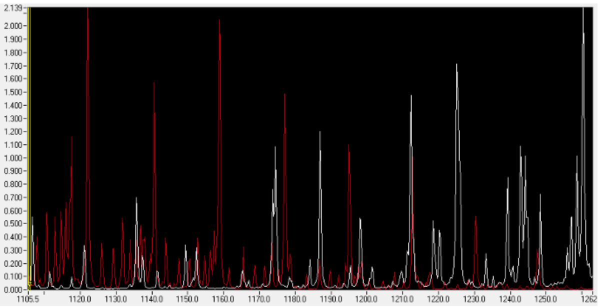

Figure 20: Absorption peaks of 30 Vol% H2O (white) against gas matrix (red)

Similar to NO a lot of the useable area is covered by other gases. Therefore just a few single peaks are used for the new calibration.

3.6 Synthetic gas mixture test

To test the new calibrations all four of them were integrated into an already used library. A test gas, which is specified in table 5, was created with the IAS HovaCal. That gas was applied to the IAG FTIR system and spectra were collected. The results of the new calibrations were plotted and compared to the known setpoints.

Carbon Monoxide	CO	1 Vol%
Carbon Dioxide	CO_2	10 Vol%
Nitrogen Monoxide	NO	3000 ppm
Nitrogen Dioxide	NO_2	200 ppm
Water	H_2O	30 Vol%
Nitrous Oxide	N_2O	100 ppm
Ammonia	NH_3	8 Vol%
Methan	CH_4	500 ppm
Propane	C_3H_8	200 ppm

Table 5: Gas composition of synthetic test gas

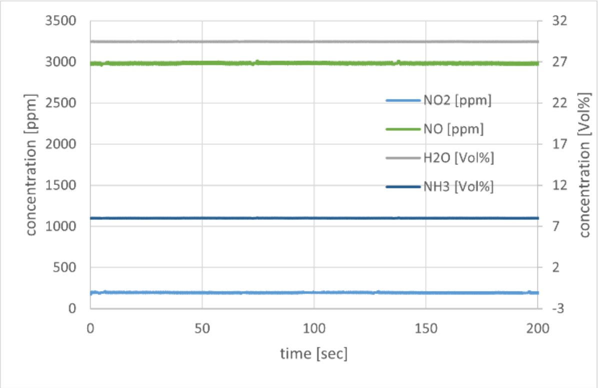

Figure 21: measurement values of 3000 ppm NO, 200 ppm NO2, 30 Vol% water and 8 Vol% ammonia

All four measured values match the expected ones so the new calibrations were included in the library and tested on the engine.

4 ENGINE DATE

Since the new calibrations work well, they we tested on a NH_3-ICE. Again, raw spectra were collected, and the improved calibrations were plotted against the original ones. The prescribed engine was used for this test.

To begin with a load variation at 900 r/min was performed. Especially NO, NO_2, H_2O and NH_3 were observed with both calibrations.

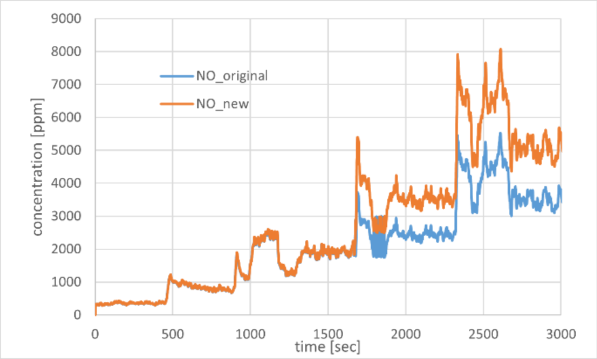

Figure 22: concentration trace of NO, original calibration (blue) against new calibration (orange)

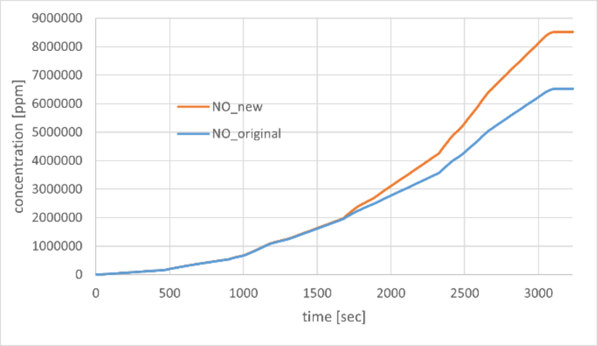

Figure 23: cumulated concentration of NO, original calibration (blue) against new calibration (orange)

As expected, the calibrations match well below 3000 ppm but differ above that level. It results in a difference of 30% relative error for cumulated concentrations.

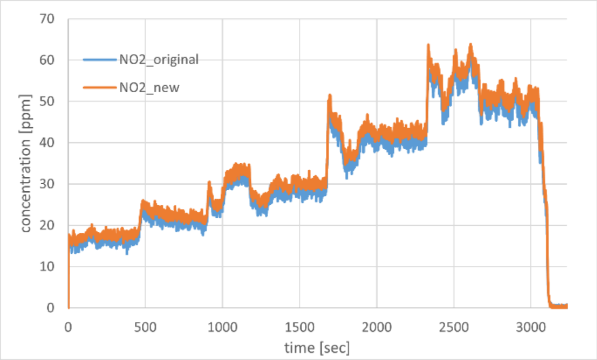

Figure 24: concentration trace of NO2, original calibration (blue) against new calibration (orange)

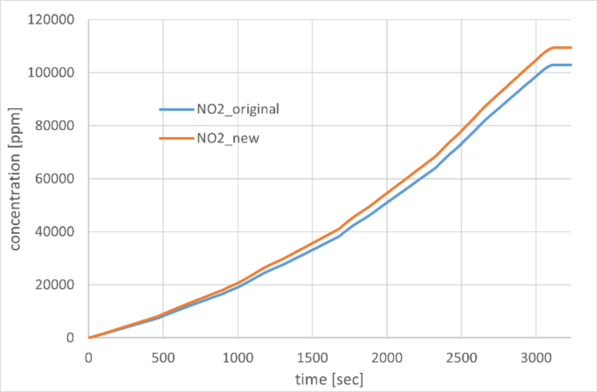

Figure 25: cumulated concentration of NO2, original calibration (blue) against new calibration (orange)

Since the original calibration already covered the measured values the results do not differ much.

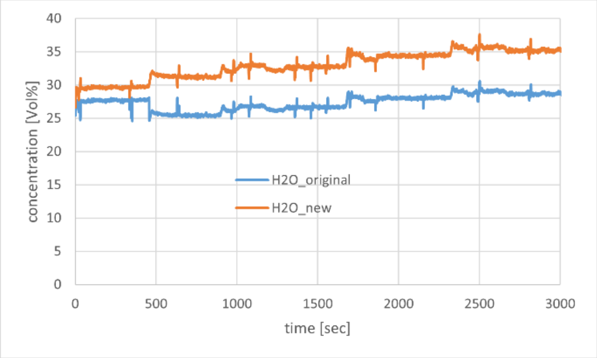

Figure 26: concentration trace of water, original calibration (blue) against new calibration (orange)

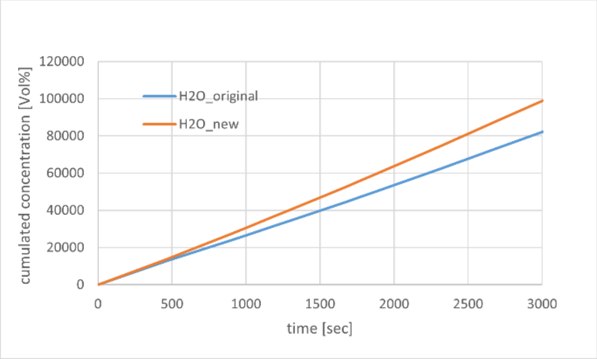

Figure 27: Cumulated concentration of water, original calibration (blue) against new calibration (orange)

Since the original range was exceeded the cumulated concentrations differ by 20% relative.

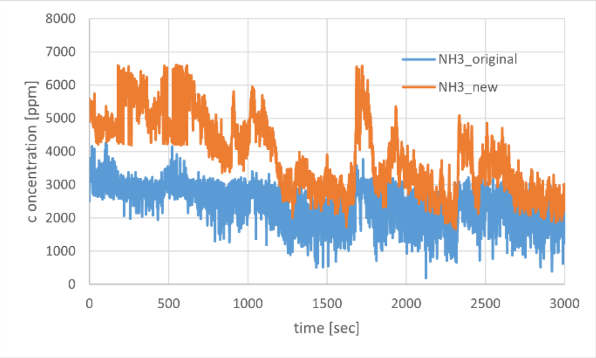

Figure 28: concentration trace of ammonia, original calibration (blue) against new calibration (orange)

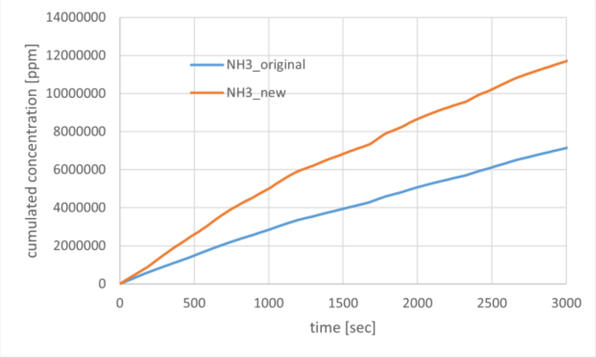

Figure 29: cumulated concentration of ammonia, original calibration (blue) against new calibration (orange)

Again, the range of the original calibration did not match the requirements. It is clearly underestimating the ammonia concentration. That leads to a total relative error of 62%.

4.1 Comparison of theoretical and measured results

To verify the results theoretical values were calculated for different Phi values.

Two cases were considered: One uses 100% ammonia as a fuel, the other one uses a 90% ammonia / 10% hydrogen mixture.

$$NH_3 + 0.75\,(O_2 + 3.76\,N_2) \rightarrow 3.32\,N_2 + 1.5\,H_2O$$

Equation 3: Ammonia combustion

$$(1 - x_{H_2})NH_3 + x_{H_2}H_2 + \frac{3-x_{H_2}}{4}(O_2 + 3.76\,N_2) \rightarrow \left(\frac{3-x_{H_2}}{2}\right)H_2O + \left(\frac{1-x_{H_2}}{2} + 3.76 * \frac{3-x_{H_2}}{4}\right)N_2$$

Equation 4: Ammonia - hydrogen combustion

Oxygen was considered to be 21 Vol% for all calculations.

Phi	nH_2O	nN_2	nH_2	nNH_3	nO_2	∑
1	1.5	3.32	0	0	0	4.82
1	1.5	3.32	0	0	0	4.82
1.1	1.5	3.37	0.15	0	0	5.02
1.1	1.5	3.32	0	0.1	0	4.92
1.2	1.5	3.42	0.3	0	0	5.22
1.2	1.5	3.32	0	0.2	0	5.02
1.3	1.5	3.47	0.45	0	0	5.42
1.3	1.5	3.32	0	0.3	0	5.12
0.9	1.35	3.27	0	0	0.08	4.70
0.8	1.2	3.22	0	0	0.15	4.57
0.7	1.05	3.17	0	0	0.23	4.45

Table 6: 100% ammonia fuel combustion

Phi	xH_2O	xN_2	xH_2	xNH_3	xO_2
1	0.31	0.69	0	0	0
1	0.31	0.69	0	0	0
1.1	0.30	0.67	0.03	0	0
1.1	0.30	0.67	0	0.02	0
1.2	0.29	0.66	0.06	0	0
1.2	0.30	0.66	0	0.04	0
1.3	0.28	0.64	0.08	0	0
1.3	0.29	0.65	0	0.06	0
0.9	0.29	0.70	0	0	0.02

0.8	0.26	0.70	0	0	0.03
0.7	0.24	0.71	0	0	0.05

Table 7: Theoretical results of 100% ammonia combustion

Phi	nH_2O	nN_2	nH_2	nNH_3	nO_2	∑
1	1.45	3.18	0	0	0	4.62
1.1	1.45	3.22	0.15	0	0	4.82
1.1	1.45	2.73	0.01	0.09	0	4.19
1.2	1.45	3.27	0.29	0	0	5.01
1.2	1.45	2.73	0.02	0.18	0	4.20
1.3	1.45	3.31	0.44	0	0	5.20
1.3	1.45	2.73	0.03	0.27	0	4.21
0.9	1.31	3.13	0	0	0.07	4.51
0.8	1.16	3.09	0	0	0.15	4.39
0.7	1.02	3.04	0	0	0.22	4.27

Table 8: 90% ammonia / 10% hydrogen fuel combustion

Phi	xH_2O	xN_2	xH_2	xNH_3	xO_2
1	0.31	0.69	0	0	0
1.1	0.30	0.67	0.03	0	0
1.1	0.35	0.65	0	0.02	0
1.2	0.29	0.65	0.06	0	0
1.2	0.35	0.65	0	0.04	0
1.3	0.28	0.64	0.08	0	0
1.3	0.34	0.65	0.01	0.06	0
0.9	0.29	0.70	0	0	0.02
0.8	0.26	0.70	0	0	0.03
0.7	0.24	0.71	0	0	0.05

Table 9: Theoretical results of 90% ammonia / 10% hydrogen combustion

First the measured water concentrations were compared against the

Fuel	Phi	H_2O [Vol%]		
(Vol% NH_3/H_2)		Theoretical	With unburnt	FTIR
100/0	1	31.1	28.5	25.1
100/0	1.2	29.9	27.9	27.7
100/0	1.3	29.3	27.3	27.8
100/0	0.9	28.7	26.2	21.8
90/10	0.9	28.9	25.9	23.8
90/10	1	31.3	28.5	26.2
90/10	1.1	34.6	31.7	27.8
90/10	1.3	34.5	32.7	29.1

Table 10: average H2O results

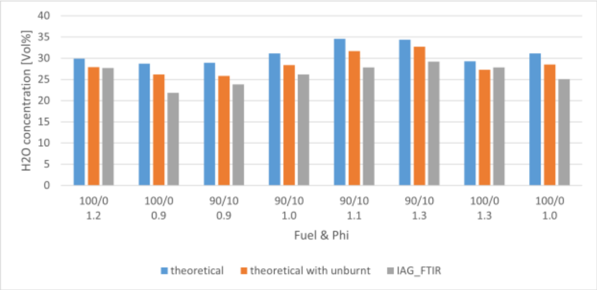

Figure 30: H2O concentration for different fuels and phi values

Table 10 and figure 30 show the calculated water concentration with and without considering unburnt ammonia as well as the measured water concentration of the FTIR. The values show good agreement for lean values but some difference for rich mixtures.

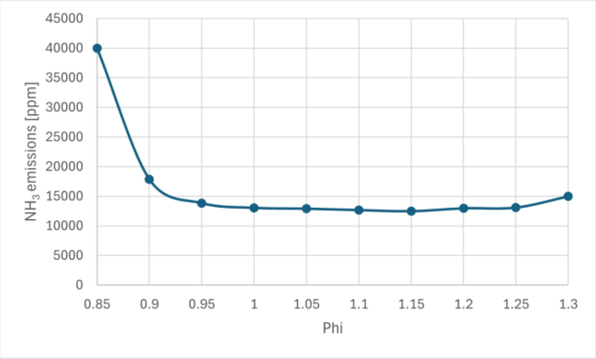

Figure 31: Ammonia emissions for different Phi values

It is clearly visible that higher amounts of unburnt ammonia are present for lean mixtures. But even for nearly stochiometric conditions around 1.2 Vol% ammonia is left, which must be considered in the design of the aftertreatment system.

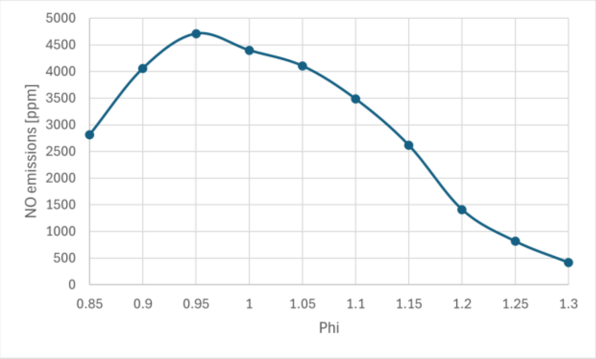

Figure 32: NO emissions for different Phi values

The highest NO emissions are present for stochiometric mixtures.

Therefore, running ammonia fueled engines at rich conditions might be the right conclusion to prevent high emissions.

5 CONCLUSIONS

The newly developed calibrations work fine for high levels of water, ammonia and nitrogen oxide. This will be an important tool if it comes to catalyst development and the improvement of the combustion process.

Further engines tests will be performed and compared to theoretical values to improve the performance.

6 REFERENCES

1. **Bocci, E., et al.** (2021). "Ammonia as a potential carbon-free fuel for internal combustion engines." *Energy Conversion and Management*, 235, 113969.

2. **Becker, R., et al.** (2020). "Ammonia combustion in internal combustion engines and the challenges of NOx and ammonia slip." *Fuel*, 276, 118097.

3. **Huang, L., et al.** (2022). "Mitigation of NOx emissions from ammonia combustion in a dual-fuel engine." *Renewable Energy*, 181, 1502-1514.

4. **He, Y., et al.** (2023). "Environmental impacts of ammonia combustion in internal combustion engines." *Environmental Science & Technology*, 57(6), 3180–3191.

5. **Kruse, L., et al.** (2020). "Exhaust gas recirculation (EGR) for ammonia combustion in internal combustion engines: A review." *Journal of Cleaner Production*, 258, 120754.

6. **Valera-Medina, A., et al.** (2018). ”Ammonia for power”. *Progress in Energy and Combustion Science,* 69, 63-102

7. **Kojima, Y., et al.** (2022). “Ammonia as a hydrogen energy carrier”. *International Journey of Hydrogen Energy,* 47/54, 22832-22839

8. **Cai, T., et al.** (2023). “Overview of fundamental kinetic mechanisms and emission mitigation in ammonia combustion”, *Chemical Engineering Journal,* 458, 141391